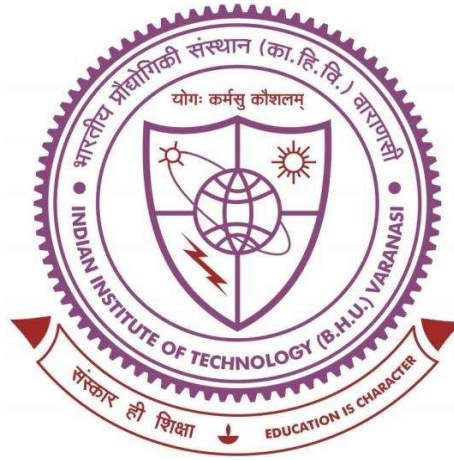


**EFFECT OF CASTING ROUTE ON TRIBOLOGICAL
PROPERTIES OF A356-Mg₂Si-TiB₂ INSITU HYBRID
COMPOSITES**



**Thesis submitted in partial fulfilment for the
Award of Degree**

Doctor of Philosophy

By

Amit Kumar Yadav

**DEPARTMENT OF METALLURGICAL ENGINEERING
INDIAN INSTITUTE OF TECHNOLOGY
(BANARAS HINDU UNIVERSITY)
VARANASI-221005
INDIA**

CERTIFICATE

It is certified that the work contained in the thesis titled "**Effect of Casting Route on Tribological Properties of A356-Mg₂Si-TiB₂ Insitu Hybrid Composites**" has been carried out under my supervision and that this work has not been submitted elsewhere for a degree.

It is further certified that the student has fulfilled all the requirements of Comprehensive Examination, Candidacy, and SOTA for the award of Ph.D. Degree.

Supervisor

Prof. Sunil Mohan

Department of Metallurgical Engineering
Indian Institute of Technology
(Banaras Hindu University)
Varanasi-221005, India

प्राचार्य / Professor

धातुकीय अभियांत्रिकी विभाग

Department of Metallurgical Engg.

भारतीय प्रौद्योगिकी संस्थान (काशी हिन्दू विश्वविद्यालय)

Indian Institute of Technology (Banaras Hindu University)

वाराणसी-221005/Varanasi-221005

DECLARATION BY THE CANDIDATE

I, "AMIT KUMAR YADAV", certify that the work embodied in this thesis is my own bonafide work and carried out by me under the supervision of "Prof. SUNIL MOHAN from "July, 2017 to June, 2023", at the "DEPARTMENT OF METALLURGICAL ENGINEERING", Indian Institute of Technology (BHU), Varanasi. The matter embodied in this thesis has not been submitted for the award of any other degree/diploma. I declare that I have faithfully acknowledged and given credits to the research work wherever their works have been cited in my work in this thesis. I further declare that I have not wilfully copied any other's work, paragraphs, text, data, results, *etc.*, reported in journals, books, magazines, reports dissertations, theses, *etc.*, or available at websites and have not included them in this thesis and have not cited as my own work.

Date 19-06-2023

Place- Varanasi



AMIT KUMAR YADAV

CERTIFICATE FROM THE SUPERVISORS

It is certified that the above statement made by the candidate is correct to the best of my/our knowledge.

Supervisor



Prof. Sunil Mohan

Department of Metallurgical Engineering
Indian Institute of Technology
(Banaras Hindu University)

Varanasi-221005

प्राचार्य / Professor

धातुक्रीय अभियांत्रिकी विभाग

Department of Metallurgical Engg.

भारतीय प्रौद्योगिकी संस्थान (काशी हिन्दू विश्वविद्यालय)

Indian Institute of Technology (Banaras Hindu University)

वाराणसी-221005/Varanasi-221005

Head



Department of Metallurgical Engineering

Indian Institute of Technology

(Banaras Hindu University)

Varanasi-221005

विभागाध्यक्ष / HEAD

धातुक्रीय अभियांत्रिकी विभाग

Department of Metallurgical Engg.

भारतीय प्रौद्योगिकी संस्थान (काशी हिन्दू विश्वविद्यालय)

Indian Institute of Technology (Banaras Hindu University)

वाराणसी-221005/Varanasi-221005

COPY RIGHT TRANSFER CERTIFICATE

Title of the Thesis: EFFECT OF CASTING ROUTE ON TRIBOLOGICAL PROPERTIES
OF A356-Mg₂Si-TiB₂ INSITU HYBRID COMPOSITES

Name of the Student: AMIT KUMAR YADAV

COPYRIGHT TRANSFER

The undersigned hereby assigns to the Indian Institute of Technology (Banaras Hindu University) Varanasi all rights under copyright that may exist in and for the above thesis submitted for the award of the "DOCTOR OF PHILOSOPHY".

Date: 19-06-2023

Place: Varanasi



(AMIT KUMAR YADAV)

Note: However, the author may reproduce or authorize others to reproduce material extracted verbatim from the thesis or derivative of the thesis for author's personal use provided that the source and the Institute's copyright notice are indicated.

*I would like to dedicate
this
Thesis*

To my

*Beloved Father
Late. Shri Lal Ji Yadav*

ACKNOWLEDGEMENT

I take this opportunity to express my sincere thanks and gratitude beyond words to my supervisor, Prof. Sunil Mohan for his consistent help, encouragement, and valuable discussions during the entire period of my research work. I would also like to extend my deep gratitude to Late. Prof. I. Chakrabarty for his guidance and encouragement during initial years of my PhD work. I would not have been able to complete the thesis without their utmost involvement and invaluable efforts. Besides my supervisors, I would like to thank Prof. K.K. Singh and Dr. J.K. Singh, Department of Metallurgical Engineering, for his insightful comments and encouragement. They motivated me to pursue research problems and the need for persistent effort to accomplish the goal. I am truly indebted to them.

I would like to extend my gratitude to the present head of the department, Prof. Sunil Mohan, and former Heads of department Prof. N.K. Mukhopadhyay and Prof. R.K. Mandal, for providing all the necessary facilities to carry out the research work. I am also thankful to Prof. R. K. Gautam, Dept of Mechanical engineering for his valuable suggestions and guidance. I have deep sense of gratitude to all other faculty members of the Department of Metallurgical Engineering, IIT (BHU), for their cooperation and inspiration.

I am also thankful to all the lab, workshop, and office staff especially Mr. J.P. Patel for their support. I would also like to extend my thanks to the Prof.-in-charge, CIFIC, and his technical team especially Mr. Girish Sahu, Mr. Sudhakar and Mr. Nirmal for providing the research facilities.

I am thankful to all my friends, Nitesh, Vineet, Ankit, Manik, Sandeep, Jaydeep, Sarika, Shanker, and seniors especially Dr. Gaurav Gautam, Dr. Ankitendran Mishra Dr. Subash Chandra Ram and Dr. Chandrasekhar Kumar. I would also like to thanks my juniors Ishwari Narayan, Dharmendra, Vikrant, Dileep and bharat for their support and making joyful and memorable moments at IIT (BHU), Varanasi.

I would like to express my deepest gratitude to my parents Srimati Shobhna Devi and Late. Shri Lal Ji Yadav, for educating me, their unconditional support and encouragement to pursue my interest. I would also like to express my sincere gratitude to my elder brothers Dr. Vijay Kumar Yadav and Mr. Pradeep Kumar Yadav and my sisters-in-law Mrs. Gita and Mrs. Krishna for their constant support. Last, but not least, I would like to offer my deep sense of gratitude to my dear wife Mrs. Bindu who always stood beside me, encouraged, and supported me through my ups and downs. I express my heartfelt appreciation to Vikas, Priyanka, Avnish, Tarun, Spana and Keerti for keeping me in good cheer with their invigorating company. I also wish to thank all my friends and the persons whose names have not been mentioned on this piece of paper for extending their co-operation directly or indirectly.



Amit Kumar Yadav

CONTENTS

ACKNOWLEDGEMENT.....	xi
LIST OF FIGURES.....	xviii
LIST OF TABLES.....	xix
LIST OF SYMBOLS.....	xxi
PREFACE.....	xxvi
CHAPTER 1: INTRODUCTION	1
1.1 INTRODUCTION	1
1.2 SCOPE OF PRESENT INVESTIGATION.....	4
1.3 OBJECTIVES OF THE PRESENT STUDY	4
CHAPTER 2: LITERATURE REVIEW	7
2.1 APPLICATION OF Al ALLOYS FOR AUTOMOTIVE COMPONENT	7
2.2 COMPOSITE MATERIALS	8
2.3 CLASSIFICATION OF COMPOSITE MATERIALS	8
2.3.1 Polymer matrix composite	8
2.3.2 Ceramic matrix composite	9
2.3.3 Metal matrix composite.....	9
2.4 FABRICATION PROCESSES OF AMCs.....	11
2.4.1 Liquid state processes	11
2.4.1.1 Stir casting.....	11
2.4.1.2 Centrifugal casting.....	12
2.4.1.3 Infiltration process.....	12
2.4.1.4 Ultrasonic-assisted casting	13
2.4.1.5 Disintegrated melt deposition (DMD).....	14
2.4.2 Solid state processes.....	14
2.4.2.1 Powder Metallurgy (PM) method.....	14

2.4.2.2 Mechanical alloying.....	15
2.4.2.3 Diffusion bonding	15
2.4.3 Semisolid processes.....	16
2.4.3.1 Thixo-casting	16
2.4.3.2 Rheo-casting	16
2.5 COOLING SLOPE (CS) CASTING.....	17
2.6 Al-Mg ₂ Si INSITU METAL MATRIX COMPOSITE	19
2.6.1 Morphology and growth mechanism of Mg ₂ Si	20
2.6.2 Influence of different processing routes on the microstructure and properties	20
2.6.2.1 Influence of intensive melt shearing	20
2.6.2.2 Influence of melt superheating treatment	21
2.6.2.3 Semi-solid processing	21
2.6.3 Effect of chemical modifications of Mg ₂ Si particles.....	22
2.6.3.1 Effect of extra silicon addition.....	22
2.6.3.2 Effect of extra Mg additions	23
2.6.3.3 Effect of TiB ₂ addition	25
2.6.3.4 Modifications of morphology with different alloying elements	25
2.6.4 Effect of solution treatment and ageing.....	30
2.7 TiB ₂ PHASE AS REINFORCEMENT	30
2.8 Al BASED HYBRID COMPOSITE.....	32
2.8.1 Microstructural and mechanical characteristics	33
2.8.2 Tribological characteristics.....	35
2.8.2.1 Wear	35
2.8.2.2 Effect of operating parameters.....	36
2.8.2.3 Friction and laws of friction.....	37
2.8.2.4 Stages of Friction	38

2.9 Al-Mg ₂ Si-TiB ₂ INSITU HYBRID COMPOSITES	41
CHAPTER 3: EXPERIMENTAL DETAILS	43
3.1 INTRODUCTION	43
3.2 MATERIALS AND METHOD	43
3.2.1 Preparation of A356-10%Mg ₂ Si composite.....	43
3.2.2 Preparation of A356-10%Mg ₂ Si-xTiB ₂ hybrid composite	44
3.3 X-RAY DIFFRACTOMETER FOR PHASE ANALYSIS	46
3.4 DENSITY AND POROSITY CALCULATIONS	46
3.5 MICROSTRUCTURAL CHARACTERIZATION.....	46
3.5.1 Optical Microscope (OM).....	47
3.5.2 Scanning Electron Microscope (SEM).....	47
3.5.3 Measurement of Particle size and shape factor	48
3.6 MECHANICAL PROPERTIES	48
3.6.1 Hardness Test.....	48
3.6.2 Tensile Test	48
3.7 TRIBOLOGICAL TEST AND WORN SURFACES ANALYSIS	49
3.7.1 Wear and friction.....	49
3.7.2 Surface Topography	50
3.8 STATISTICAL MODELLING USING RESPONSE SURFACE METHODOLOGY	50
CHAPTER 4: MICROSTRUCTURAL CHARACTERIZATION AND MECHANICAL PROPERTIES OF A356-Mg₂Si-TiB₂ COMPOSITES	53
4.1 INTRODUCTION	53
4.2 CHEMICAL COMPOSITION of A356 ALLOY	53
4.3 X-RAY DIFFRACTION (XRD) ANALYSIS	53
4.4 MICROSTRUCTURAL AND MECHANICAL CHARACTERISTICS OF HYBRID COMPOSITES IN STIR CAST CONDITIONS.....	54
4.4.1 Density and Porosity measurement.....	54

4.4.2 Optical microscopy.....	56
4.4.3 Scanning electron microscopy.....	58
4.4.4 Elemental analysis and particle size & their distribution	60
4.4.5 Hardness Properties	61
4.4.6 Tensile properties	62
4.5 MICROSTRUCTURAL AND MECHANICAL CHARACTERISTICS OF HYBRID COMPOSITES IN COOLING SLOPE CAST CONDITIONS	65
4.5.1 Density and porosity measurement.....	65
4.5.2 Optical microscopy.....	66
4.5.3 Scanning electron microscopy.....	68
4.5.4 Particle size analysis.....	70
4.5.5 Hardness	72
4.5.6 Tensile properties	73
4.6 COMPARATIVE STUDY OF MICROSTRUCTURAL FEATURES AND MECHANICAL PROPERTIES OF STIR CAST AND CS CAST COMPOSITES ..	77
4.6.1 Microstructural features.....	77
4.6.2 Mechanical properties.....	79
4.7 Summary	81
CHAPTER 5: TRIBOLOGICAL CHARACTERISTICS OF STIR CAST A356- Mg₂Si-TiB₂ HYBRID COMPOSITE.....	83
5.1 INTRODUCTION.....	83
5.2 WEAR & FRICTION BEHAVIOR UNDER DRY SLIDING.....	83
5.2.1 Influence of Sliding Distance	83
5.2.2 Influence of Load.....	88
5.2.3 Influence of Sliding Velocity	94
5.2.4 Influence of TiB ₂ Content.....	97
5.3 Wear Debris Analysis.....	102
5.4 Summary	104

CHAPTER 6: TRIBOLOGICAL CHARACTERISTICS OF CS CAST A356-Mg₂Si-TiB₂ HYBRID COMPOSITE	105
6.1 INTRODUCTION	105
6.2 WEAR & FRICTION BEHAVIOR UNDER DRY SLIDING	105
6.2.1 Influence of Sliding Distance.....	105
6.2.2 Influence of Load	110
6.2.3 Influence of Sliding Velocity	114
6.2.4 Influence of TiB ₂ Amount.....	118
6.3 COMPARATIVE STUDY OF TRIBOLOGICAL PROPERTIES OF STIR CAST AND CS CAST HYBRID COMPOSITES	123
6.4 Summary.....	125
CHAPTER 7: STATISTICAL MODELLING OF TRIBOLOGICAL PARAMETERS USING RESPONSE SURFACE METHODOLOGY	129
7.1 INTRODUCTION	129
7.2 STATISTICAL MODELLING OF WEAR RATE AND COF OF STIR CAST HYBRID COMPOSITES	130
7.2.1 Central composite design (CCD)	130
7.2.2 Quadratic model and analysis of variance	131
7.2.3 ANOVA for wear rate and COF of quadratic model	132
7.2.4 Regression equation for wear rate and COF	133
7.2.5 Optimization of tribological parameters	139
7.3 STATISTICAL MODELLING OF WEAR RATE AND COF OF COOLING SLOPE CAST HYBRID COMPOSITES.....	141
7.3.1 Central composite design (CCD)	141
7.3.2 Quadratic model and analysis of variance	142
7.3.3 Regression equation for wear rate and COF	145
7.3.4 Optimization of tribological parameters	153
7.4 Summary.....	154

CHAPTER 8: MAJOR CONCLUSION.....157
SUGGESTIONS FOR FUTURE WORK.....158
REFERENCES.....159

LIST OF FIGURES

Fig. 2.1 Schematic diagram of cooling slope casting set up	18
Fig. 3.1 Schematic diagram of CS casting set up.....	45
Fig. 3.2 (a) Location of test sample from casting (b) Image of the castings.....	47
Fig. 4.1 XRD patterns of base alloy (A356) and A356-10Mg ₂ Si-xTiB ₂ composites (x= 0, 1, 3 and 5).....	54
Fig. 4.2 (a) Theoretical and actual density and (b) average porosity percentage of A356 alloy and stir cast composites	55
Fig. 4.3 Optical micrograph of matrix A356 alloy.....	56
Fig. 4.4 Optical micrographs of A356-10Mg ₂ Si-xTiB ₂ composites (a) x= 0, (b) x= 1, (c) x= 3 and (d) x= 5.....	57
Fig. 4.5 SEM micrographs of A356-10Mg ₂ Si-xTiB ₂ composites with varying content of TiB ₂ particles (a) x= 0, (b) x= 1, (c) x= 3 and (d) x= 5	58
Fig. 4.6 SEM micrographs of A356-10Mg ₂ Si-3TiB ₂ hybrid composites at (a) low magnification (b) high magnification (c) point of EDS in SEM image of A356-10Mg ₂ Si-3TiB ₂ and (d) corresponding EDS spectrum	59
Fig. 4.7 SEM micrograph of A356-10Mg ₂ Si-3TiB ₂ hybrid composites and corresponding mapping of elements Al, Si, Mg, Ti and B.....	60
Fig. 4.8 Average particle size of primary Mg ₂ Si and eutectic Mg ₂ Si phase in different composites	61
Fig. 4.9 The TiB ₂ particles size distribution histogram in hybrid composite.....	61
Fig. 4.10 Hardness of A356 alloy and composites.....	62
Fig. 4.11 Engineering stress-strain curve A356 alloy, A356-10Mg ₂ Si, and A356-10Mg ₂ Si-xTiB ₂ composites	63

Fig. 4.12 Tensile strength and percentage elongation of A356 alloy, A356-10Mg ₂ Si, and A356-10Mg ₂ Si-xTiB ₂ composites	63
Fig. 4.13 Fracture surface of base alloy (a) A356 (b) A356-10Mg ₂ Si composite and hybrid composite A356-10Mg ₂ Si-xTiB ₂ with varying TiB ₂ content (c) x= 1 (d) x= 3 (e) x= 5	64
Fig. 4.14 (a) Theoretical and actual density and (b) average porosity percentage of CS cast A356 alloy and composites.....	66
Fig. 4.15 Optical micrographs of hybrid composites A356-10Mg ₂ Si-xTiB ₂ with varying content of TiB ₂ particles (a) x= 0 (b) x= 1 (c) x= 3 (d) x= 5	67
Fig. 4.16 SEM micrographs of hybrid composites A356-10Mg ₂ Si-xTiB ₂ with varying content of TiB ₂ particles (a) x= 0 (b) x= 1 (c) x= 3 (d) x= 5	69
Fig. 4.17 SEM micrographs of hybrid composites A356-10Mg ₂ Si-xTiB ₂ (a) and (c), EDS spectrum of the corresponding points in micrograph (b) and (d) respectively	71
Fig. 4.18 (a) Average particle size of α -Al, primary Mg ₂ Si and eutectic Mg ₂ Si composites in A356-10Mg ₂ Si-xTiB ₂ with varying content of TiB ₂ particles (b) TiB ₂ particle size distribution in A356-10Mg ₂ Si-5TiB ₂	72
Fig. 4.19 Vickers hardness of A356 alloy and A356-10Mg ₂ Si-xTiB ₂ composites	73
Fig. 4.20 (a) Engineering stress-strain curve and (b) Tensile strength and percentage elongation of A356 alloy, A356-10Mg ₂ Si, and A356-10Mg ₂ Si-xTiB ₂ composites.....	75
Fig. 4.21 Fractography of (a) matrix A356 (b) A356-10Mg ₂ Si composite and hybrid composite A356-10Mg ₂ Si-xTiB ₂ with varying TiB ₂ content (c) x= 1 (d) x= 3 (e) x= 5	76
Fig. 4.22 (a) Average particle size of primary Mg ₂ Si and (b) eutectic Mg ₂ Si phase in stir cast and CS cast composites	78
Fig. 4.23 The TiB ₂ particles size distribution in A356-10Mg ₂ Si-5TiB ₂ hybrid composite	79

Fig. 4.24 Vickers hardness of A356 alloy and A356-10Mg ₂ Si-xTiB ₂ composites.....	80
Fig. 4.25 (a) Tensile strength and (b) percentage elongation of A356 alloy, A356-10Mg ₂ Si, and A356-10Mg ₂ Si-xTiB ₂ hybrid composites	81
Fig. 5.1 Influence of sliding distance on wear volume at various applied loads (a) 10 N (b) 20 N (c) 30 N (d) 40 N.....	85
Fig. 5.2 Influence of sliding distance on wear rate at a fixed applied load of 30 N.....	85
Fig. 5.3 Influence of sliding distance on COF at various applied loads (a) 10 N (b) 20 N (c) 30 N (d) 40 N	86
Fig. 5.4 SEM images of worn surface of A356-10Mg ₂ Si-3TiB ₂ hybrid composite at load of 30 N and sliding distance of (a) 1000 m (b) 2000 m (c) 3000 m (d) 4000 m	87
Fig. 5.5 AFM image of A356-10Mg ₂ Si-3TiB ₂ hybrid composite at 30 N load and sliding distance of (a) 1000 m (b) 2000 m (c) 3000 m (d) 4000 m	88
Fig. 5.6 Influence of applied load on wear rate at sliding distance of (a) 1000 m (b) 2000 m (c) 3000 m (d) 4000m.....	89
Fig. 5.7 Influence of applied load on COF at sliding distance of (a) 1000 m (b) 2000 m (c) 3000 m (d) 4000 m.....	90
Fig. 5.8 Influence of applied load on specific wear rate at sliding distance of 3000m..	91
Fig. 5.9 SEM images of worn surface of A356-10Mg ₂ Si-3TiB ₂ hybrid composite at 3000 m of sliding distance and applied load of (a) 10 N (b) 20 N (c) 30 N (d) 40 N	92
Fig. 5.10 (a) SEM image of hybrid composite (C3) worn surface at applied load 30 N, (b) EDS spectrum of whole area of SEM image.	93
Fig. 5.11 AFM image of A356-10Mg ₂ Si-3TiB ₂ hybrid composite at 3000 m of sliding distance and applied load of (a) 10 N (b) 20 N (c) 30 N (d) 40 N	93
Fig. 5.12 Influence of sliding distance on wear rate at sliding distance of 1000 m and different applied loads (a) 10 N (b) 20 N (c) 30 N (d) 40 N	94

Fig. 5.13 Influence of sliding distance on COF at sliding distance of 1000 m and different applied loads (a) 10 N (b) 20 N (c) 30 N (d) 40 N.....	95
Fig. 5.14 SEM image of worn surface of A356-10Mg ₂ Si-3TiB ₂ hybrid composite at 30N applied load and different sliding speed of (a) 0.75 m/s (b) 1.5 m/s (c) 2.25 m/s and (d) 3 m/s	96
Fig. 5.15 AFM image of A356-10Mg ₂ Si-3TiB ₂ hybrid composite at sliding speed of (a) 0.75 m/s (b) 1.5 m/s (c) 2.25 m/s (d) 3 m/s.....	97
Fig. 5.16 Influence of TiB ₂ content on wear rate at constant sliding velocity of 1.5 m/s and different sliding distance of (a) 1000 m (b) 2000 m (c) 3000 m (d) 4000 m.....	98
Fig. 5.17 Influence of TiB ₂ content on COF at constant sliding velocity of 1.5 m/s and different sliding distance of (a) 1000 m (b) 2000 m (c) 3000 m (d) 4000	99
Fig. 5.18 Influence of TiB ₂ content on wear coefficient at constant sliding distance of 3000 m	100
Fig. 5.19 SEM images of worn surface at 30 N load and 3000 m of sliding distance for (a) A356 alloy and A356-10Mg ₂ Si-xTiB ₂ hybrid composite (b) x = 0 (c) x = 1 (d) x = 3 (e) x = 5.....	101
Fig. 5.20 AFM images of worn surface at 30 N load and 3000 m of sliding distance for (a) A356 alloy and A356-10Mg ₂ Si-xTiB ₂ hybrid composite (b) x = 0 (c) x = 1 (d) x = 3 (e) x = 5.....	102
Fig. 5.21 (a) SEM micrograph of Wear debris of hybrid composite at applied load 40 N and corresponding EDS spectrum of whole area and points of SEM image.	103
Fig. 6.1 Influence of sliding distance on wear volume at different applied loads (a) 10 N (b) 20 N (c) 30 N (d) 40 N	106
Fig. 6.2 Influence of sliding distance on wear rate at applied loads 30 N.....	107

Fig. 6.3 Influence of sliding distance on COF at different applied loads (a) 10 N (b) 20 N (c) 30 N (d) 40 N	108
Fig. 6.4 SEM images of worn surface of A356-10Mg ₂ Si-3TiB ₂ hybrid composite at 30 N load and sliding distance of (a) 1000 m (b) 2000 m (c) 3000 m (d) 4000 m.....	109
Fig. 6.5 AFM image of A356-10Mg ₂ Si-3TiB ₂ hybrid composite at 30 N load and sliding distance of (a) 1000 m (b) 2000 m (c) 3000 m (d) 4000 m	109
Fig. 6.6 Influence of applied load on wear rate at sliding distance of (a) 1000 m (b) 2000 m (c) 3000 m (d) 4000m.....	111
Fig. 6.7 Influence of applied load on specific wear rate at sliding distance of 3000m	111
Fig. 6.8 Influence of applied load on COF at sliding distance (a) 1000 m (b) 2000 m (c) 3000 m (d) 4000 m	112
Fig. 6.9 SEM images of worn surface of A356-10Mg ₂ Si-3TiB ₂ hybrid composite at 3000 m of sliding distance and applied load of (a) 10 N (b) 20 N (c) 30 N (d) 40 N ..	113
Fig. 6.10 (a) SEM micrograph of worn surface A356-10Mg ₂ Si-3TiB ₂ hybrid composite at applied load 30 N, (b) EDS spectrum of whole area of SEM micrograph	114
Fig. 6.11 AFM image of A356-10Mg ₂ Si-3TiB ₂ hybrid composite at 3000 m of sliding distance and applied load of (a) 10 N (b) 20 N (c) 30 N (d) 40 N	114
Fig. 6.12 Influence of sliding velocity on wear rate at sliding velocity of 1000 m and different applied loads (a) 10 N (b) 20 N (c) 30 N (d) 40 N	115
Fig. 6.13 Influence of sliding velocity on COF at sliding distance of 1000 m and different applied loads (a) 10 N (b) 20 N (c) 30 N (d) 40 N	116
Fig. 6.14 SEM image of worn surface of A356-10Mg ₂ Si-3TiB ₂ hybrid composite at 30 N load and 1000 m of sliding distance and sliding velocity of (a) 0.75 m/s (b) 1.5 m/s (c) 2.25 m/s (d) 3 m/s	117

Fig. 6.15 AFM image of A356-10Mg ₂ Si-3TiB ₂ hybrid composite at 30 N load and 1000 m of sliding distance and sliding velocity of (a) 0.75 m/s (b) 1.5 m/s (c) 2.25 m/s (d) 3 m/s	117
Fig. 6.16 Influence of TiB ₂ content on wear rate at constant sliding velocity of 1.5 m/s and different sliding distance of (a) 1000 m (b) 2000 m (c) 3000 m (d) 4000 m	119
Fig. 6.17 Influence of TiB ₂ content on COF at constant sliding velocity of 1.5 m/s and different sliding distance of (a) 1000 m (b) 2000 m (c) 3000 m (d) 4000 m	120
Fig. 6.18 Influence of TiB ₂ content on wear coefficient at constant sliding distance of 3000 m	120
Fig. 6.19 SEM images of worn surface at 30 N load and 3000 m of sliding distance for (a) A356 alloy and A356-10Mg ₂ Si-xTiB ₂ hybrid composite (b) x = 0 (c) x = 1 (d) x = 3 (e) x = 5	121
Fig. 6.20 Wear debris of A356-10Mg ₂ Si-3TiB ₂ hybrid composite at applied load of (a) 20 N and (b) 40 N	122
Fig. 6.21 AFM images of worn surface at 30 N load and 3000 m of sliding distance for (a) A356 alloy and A356-10Mg ₂ Si-xTiB ₂ hybrid composite (b) x = 0 (c) x = 1 (d) x = 3 (e) x = 5	122
Fig. 6.22 Comparison of wear rate and COF of stir cast and CS cast base alloy and composites at fixed load, sliding distance and velocity	124
Fig. 7.1 Surface and contour plots for predicting the wear rate (a) applied load vs sliding distance, (b) applied load vs wt.% of TiB ₂ and (c) sliding distance vs wt.% of TiB ₂	135
Fig. 7.2 Surface and contour plots for COF (a) load vs sliding distance, (b) load vs wt.% of TiB ₂ , and (c) sliding distance vs wt.% of TiB ₂	136

Fig. 7.3 Comparison of experimental and predicted values and normal probability for residuals of wear rate.....	137
Fig. 7.4 Comparison of experimental and predicted values and normal probability for residuals of COF.....	138
Fig. 7.5 Desirability graph of optimum parameters for wear rate.....	140
Fig. 7.6 Desirability graph of optimum parameters for COF.....	140
Fig. 7.7 Contour and surface plots for wear rate.....	148
Fig. 7.8 Contour and surface plots for COF.....	150
Fig. 7.9 Predicted versus actual plots, normal probability of residual and residuals against the run order for wear rate.....	151
Fig. 7.10 Predicted versus actual plots, normal probability of residual and residuals against the run order for COF.....	152
Fig. 7.11 Ramp function graph of Desirability for A356-10Mg ₂ Si-xTiB ₂ hybrid composite.....	153

LIST OF TABLES

Table 3.1 Composites with varying TiB ₂ content.....	45
Table 3.2 Sliding wear parameters with their levels used in RSM.....	51
Table 4.1 Elemental composition of A356 alloy	53
Table 7.1 Input levels of sliding wear parameters	130
Table 7.2 Design matrix and experimental wear rate and COF.....	130
Table 7.3 ANOVA for wear rate	132
Table 7.4 ANOVA for COF	132
Table 7.5 Experimental and Predicted values of the model for optimal wear	140
Table 7.6 Experimental and Predicted values of the model for optimal COF	140
Table 7.7 Sliding wear parameters with their levels.....	141
Table 7.8 Design matrix and experimental results of wear rate and COF	141
Table 7.9 Statistics model summary for wear rate.....	143
Table 7.10 Statistics model summary for COF.....	143
Table 7.11 ANOVA for wear rate	143
Table 7.12 ANOVA for COF	144
Table 7.13 Experimental and Predicted values of the model for optimal wear rate and COF	154

LIST OF SYMBOLS

1. Abbreviation

Al	Aluminium
Si	Silicon
Mg	Magnesium
Ti	Titanium
B	Boron
Cu	Copper
Fe	Iron
Zn	Zinc
Mn	Manganese
Ni	Nickel
Cr	Chromium
W	Tungsten
Sn	Tin
Sr	Strontium
Gr	Graphite
Mg ₂ Si	Magnesium Silicide
TiB ₂	Titanium boride
Al ₃ Ti	Titanium aluminide
AlB ₂	Aluminium boride
ZrB ₂	Zirconium boride
Al ₃ Zr	Zirconium aluminide
N	Newton
m	meter
cm	Centimetre
mm	millimetre
μm	Micron
gm	gram
α-Al	Aluminium phase
ε	metastable phase

η	Supersaturated phase
ρ	Density
Vol.%	Volume percentage
Wt.%	Weight percentage
MPa	Mega Pascal
HV	Vickers's Hardness
$^{\circ}\text{C}$	Degree centigrade
Sec	Second

2. Acronyms

A356	Al-Si-Mg alloy
AMCs	Al matrix composites
MMCs	Metal matrix composites
PMCs	Polymer matrix composites
CMCs	Ceramic matrix composites
ASTM	American society for testing and materials
VHN	Vickers's hardness number
RSM	Response Surface Methodology
CCD	Centre Composite Design
DOE	Design of Expert
ANN	Artificial Neural Network
UTS	Ultimate tensile strength
YS	Yield Strength
XRD	X-ray Diffraction
OM	Optical microstructure
SEM	Scanning Electron Microscopy
EDS	Energy Dispersive X-ray Spectroscopy
TEM	Transmission Electron Microscopy
AFM	Atomic force microscope

PREFACE

The demand of lightweight and high strength materials is increasing in automotive, aerospace and transportation applications due to strict environmental regulations and high fuel prices. The global need is to have fuel-efficient vehicles for energy conservation. There is a wide range of components such as cylinder blocks, cylinder liners, pistons, brake drums, connecting rods, etc., where we need materials with higher mechanical and tribological properties. But the conventional materials do not fulfil such requirements, composites can be tailored to provide combination of required properties with suitable choice of matrix and reinforcement. Apart from the monolithic composites, hybrid composites can be developed to meet the specific properties.

Hybrid composites are fabricated using two or more reinforcing material into metal matrix, offering more flexibility and reliability for engineering components. Properties of hybrid composite can be easily controlled by taking a suitable combination and composition of reinforcement particles. Hybrid composites have better properties than mono composites because they combine the advantages of more than one constituent reinforcement.

Al based composites can be produced by either exsitu process or insitu process. In exsitu process externally synthesized particulates added into the matrix, whereas in insitu process particulate are synthesized in matrix during fabrication. However, insitu technique have several advantages over exsitu technique such as homogeneous distribution of particulates, thermodynamically stable phase, good interfacial bonding with the matrix. Stir casting and cooling slope casting process can be the potential fabrication methods of composites due to its simplicity, low operation cost and near net shape forming capabilities.

The present investigation involves the synthesis of A356-Mg₂Si-TiB₂ hybrid composites with fixed 10wt.% of Mg₂Si and varying wt.% of TiB₂ reinforcement with 0, 1, 3 and 5 wt.% by stir casting and cooling slope (CS) casting route. The stir and CS cast hybrid composites were characterized for microstructural and consequent mechanical and tribological properties. Present thesis has been given in 8 chapters:

Chapter 1: This chapter provides an overview of the problem, as well as the scope and objectives of the investigations.

Chapter 2: This chapter presents literature reviews on the advancement of Al alloys and composites for automotive applications and their advantages and disadvantages, how Al based hybrid composites could be an alternative material for such applications. It describes various types of composites, metal matrix composites (MMCs), their advantages, applications, and fabrication methods with various matrices and reinforcements. It also describes insitu Mg₂Si reinforced composites, the growth morphology of the Mg₂Si reinforcements, different processing for refinement and modification of Mg₂Si reinforcement. Subsequently, presents the state of the knowledge about the microstructural, mechanical and tribological properties of various Al based hybrid composites.

Chapter 3: This chapter elaborates on the experimental techniques and instruments used to characterize the composites. The fabrication of A356-Mg₂Si-TiB₂ hybrid composite by stir casting and CS casting techniques with varying TiB₂ content. The hybrid composites have been characterized by X-ray diffraction, optical and scanning electron microscopy. Subsequently, the hardness, tensile and tribological properties have been evaluated.

Chapter 4: It deals with the microstructural characterization and mechanical properties of the hybrid composite with varying TiB_2 particles fabricated by stir casting and CS casting routes have been presented. It comprises XRD analysis data and interpretation for phase identification. It reveals three phases, Al, Mg_2Si and TiB_2 , are present in the hybrid composites. Microstructural characteristics were studied using an optical microscope and scanning electron microscope. It shows that refinement of primary and eutectic Mg_2Si phase on the incorporation of TiB_2 particles as it acts as heterogeneous nuclei for the Mg_2Si phase. Applying the CS casting further improve the refinement and modification of phase morphology of the Mg_2Si and matrix phase owing to shearing action of the cooling slope and fragmentation of dendrites. CS casting technique also improve the distribution of Mg_2Si and TiB_2 particles in the hybrid composites. Mechanical test results indicate improvement in strength parameters such as ultimate tensile strength (UTS) and ductility with increased wt.% of TiB_2 particles. The behaviour of tensile fracture has been explained based on characteristics in fractography.

Chapter 5: This chapter includes the tribological behaviour of stir cast hybrid composites in dry sliding conditions. It was found that wear rate increases with increasing load and sliding distance. Increasing TiB_2 content in hybrid composites wear rate decreases while coefficient of friction increases and hybrid composite having 5 wt.% TiB_2 particles shows the minimum wear rate. The worn surfaces were examined using SEM attached with EDS and AFM. At low applied load and sliding distance mild/oxidative wear mode is dominant whereas at high applied load and sliding distance delamination is dominant wear mechanism. AFM analysis indicate that increasing TiB_2 content in hybrid composite surface roughness of worn surfaces decreases.

Chapter 6: This chapter presents the tribological behaviour of CS cast hybrid composites. Tribological properties of CS cast hybrid composites examined under

varying applied load, sliding distance, sliding velocity, and varying wt.% of TiB₂. It has been found that CS cast hybrid composite have better wear resistance properties as compare to the stir cast hybrid composites. However, it was interesting to note that applying CS casting process, COF values also decreased even with an increase in TiB₂ content up to 3 wt.% of TiB₂. It could be due to higher matrix and Mg₂Si phase refinement and better dispersion of reinforcements in the CS cast hybrid composites. Worn surfaces have been inspected using SEM and AFM and observed that abrasive wear is dominant wear mechanism at low applied load and sliding distance while plastic deformation and delamination is the dominant wear mechanism at higher load and sliding distance. AFM analysis reveals that lower surface roughness values even at higher load and sliding distance.

Chapter 7 This chapter presents the statistical modelling and optimization of tribological parameters of stir cast and CS cast hybrid composites using Response Surface Methodology (RSM). Design expert 13 software was used to optimize the response (wear rate and COF). Central composite design (CCD) is used to design the experiment. For analysis of wear rate and COF, quadratic model is suggested from fit summary as the R² value very close to 1. Analysis of variance (ANOVA) is used to check the significance, and p-value less than 0.05 and lack of fit insignificant specifies the adequacy of the developed model. Contour and surface plot for RSM is given to see the behaviour of wear rate and COF with varying input parameters and obtained results are in agreement with experimental results. Predicted and experimental values of wear rate and COF are found to be very close in the confirmatory test, also confirms that this model can be adequate for prediction of wear rate and COF.

Chapter 8: It includes the conclusions drawn from the current investigation as well as recommendations for the future scope.